Author(s): Robertson, Stuart; Chivers, Tristram; Tuononen, Heikki

Title: Experimental and Theoretical Investigations of the Contact Ion Pairs Formed by Reactions of the Anions [(EPR2)2N]− (R = iPr, tBu; E = S, Se) with the Cations [(TePR2)2N]+ (R = iPr, tBu)

Year: 2009

Version:

Please cite the original version:

Robertson, S., Chivers, T., & Tuononen, H. (2009). Experimental and Theoretical Investigations of the Contact Ion Pairs Formed by Reactions of the Anions [(EPR2)2N]− (R = iPr, tBu; E = S, Se) with the Cations [(TePR2)2N]+ (R = iPr, tBu). Inorganic Chemistry, 48(14), 6755-6762. https://doi.org/10.1021/ic900703e

Experimental and Theoretical Investigations of the Contact Ion Pairs Formed by Reaction of the Anions $[(EPR_2)_2N]^-$ (R = ^{i}Pr, ^{t}Bu; E = S, Se) with the Cations $[(TePR_2)_2N]^+$ (R = ^{i}Pr, ^{t}Bu)

Stuart D. Robertson,[†] Tristram Chivers*,[†] and Heikki M. Tuononen[‡]

Department of Chemistry, University of Calgary, 2500 University Drive NW, Calgary, T2N 1N4, Alberta, Canada, and Department of Chemistry, University of Jyväskylä, P.O. Box 35, FI-40014 Jyväskylä, Finland

---

* To whom correspondence should be addressed.

E-mail: chivers@ucalgary.ca

Telephone: (403) 220-5741

Fax: (403) 289-9488

† University of Calgary

‡ University of Jyväskylä

Abstract

The reactions of the sodium salts $[(EPR_2)_2N]Na(TMEDA)$ (R = ^{i}Pr, ^{t}Bu; E = S, Se) with the iodide salts $[(TePR_2)_2N]I$ (R = ^{i}Pr, ^{t}Bu) in toluene produce the mixed chalcogen systems $[(EPR_2)_2N][(TePR_2)_2N]$ (**6b**, E = Se, R = ^{t}Bu; **6c**, E = S, R = ^{t}Bu; **7b**, E = Se, R = ^{i}Pr; **7c**, E = S, R = ^{i}Pr). Compounds **6b, 6c**, **7b** and **7c** have been characterized in solution by variable temperature multinuclear (^{31}P, ^{77}Se and ^{125}Te) NMR spectroscopy and in the solid state by single crystal X-ray crystallography. The structures are comprised of contact ion pairs linked by bonds between tellurium and sulfur or selenium atoms. For the tert-butyl derivatives **6b** and **6c** the anionic half of the molecule is coordinated in a bidentate (E,E′) fashion to one tellurium atom of the cationic half to give a spirocycle, whereas in the *iso*-propyl derivatives **7b** and **7c** the anion acts as a monodentate ligand with only one E-Te bond and the second sulfur or selenium atom pointing away from the cation. Comparison of the chalcogen-chalcogen bond orders in **6b**, **6c**, and the all-tellurium system **6a** (E = Te), as determined from the experimental bond lengths, shows that the Te-Te bond order in the cations decreases as the strength of the E-Te interaction increases. This trend is attributed to increased electron donation from the anion into the LUMO [σ*(Te-Te)] of the cation along the series S < Se < Te. A similar trend is observed for the monodentate contact ion pairs **7b** and **7c**. Density functional theory calculations provided information about the relative energies of bidentate and monodentate contact ion pair structures and the extent of intramolecular electron transfer in these systems.

Introduction

Chalcogen-centered ligands of the type **1** (E = chalcogen), i.e. dichalcogenidoimidodiphosphinates, have attracted a great deal of attention since their original discovery by Schmidpeter 45 years ago.[1,2] In the case of E = O, S, Se these monoanions are readily accessible by deprotonation of the corresponding imides and a large variety is available as a consequence of varying the chalcogen atoms and/or the organic groups bound to phosphorus. The primary focus has been the coordination chemistry of these bidentate ligands, and several reviews that provide details of the complexes of **1** with a diverse array of main group, lanthanide and transition metals have been published.[3-5] A significant recent application of these complexes, particularly in the case of the selenium derivative (**1**, E = Se, R = ^{i}Pr), has been as single-source precursors for the generation of metal selenides in the form of semiconducting thin films [6-17] or quantum dots[18] via CVD or solvothermal processes.

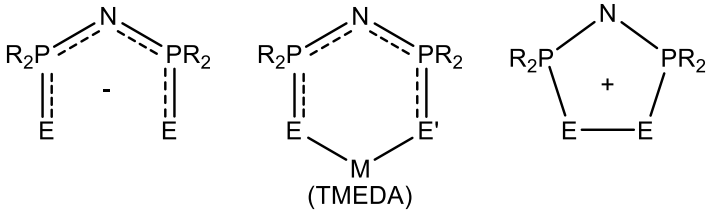

(**1**) (**2**) (**3**)

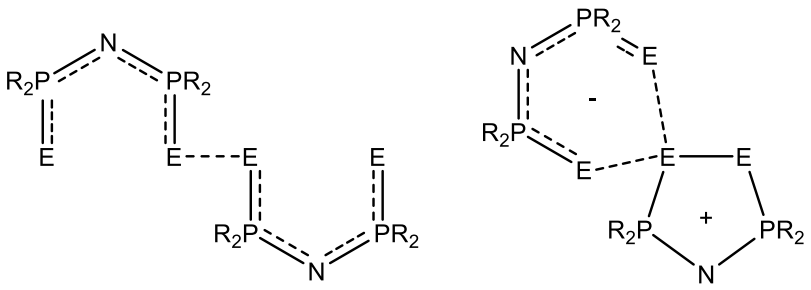

(**4**) (**5**)

The success of this approach to binary metal selenides provided the impetus to develop a synthesis of the tellurium analogues (**1**, E = Te) with the anticipation that the corresponding metal complexes would serve as single-source precursors to metal tellurides. Unlike the lighter dichalcogenido congeners (**1**, E = S, Se), the N-protonated derivatives of the ditellurido ligands cannot be prepared by direct oxidation of $R_2PN(H)PR_2$ with tellurium. However, deprotonation of the PNP backbone in these P(III)/P(III) systems with sodium hydride *prior to* oxidation with tellurium affords these ligands as sodium salts (**2**, E = E' = Te; R = Ph, ^{i}Pr; M = Na).[19, 20] The coordination chemistry of the *iso*-propyl derivative has subsequently been studied with a variety of main group,[20, 21] transition[21-24] and f-block[25, 26] metals. New structural arrangements have been observed, compared to those observed for the metal complexes of **1** (E = S, Se), especially for the coinage metals, as a result of the propensity of **1** (E = Te) to act as a doubly bridging ligand.[22] Several of these complexes have been successfully employed as single source precursors to binary metal tellurides, e.g. CdTe,[27] In_2Te_3,[28] Sb_2Te_3[29] and PbTe.[30] Very recently, the conditions for the optimal syntheses of lithium derivatives of *hetero*dichalcogenidoimidodiphosphinates containing tellurium and either sulfur or selenium (**2**, E = Te, E' = S, Se; R = ^{i}Pr; M = Li) were reported.[31] These novel reagents were subsequently used in metathesis reactions to prepare homoleptic complexes with group 10 metals.[32, 33]

In addition to coordination complexes, a new aspect of the chemistry of anions of the type **1**, *viz*. redox behavior, has been comprehensively investigated. Two-electron oxidation of these anions with iodine yields a variety of cations of the type **3**, which contain a puckered five-membered ring.[34] When a coordinating counter-anion such as I^-

is present, elongation of the E-E bond in the cation is observed. On the basis of density functional theory (DFT) calculations this elongation has been attributed to donation of electron density from a lone pair of the iodide anion into the LUMO of the cation, which is the σ^*(E-E) orbital. Such bond elongation is not evident in ion-separated salts containing non-interacting SbF_6^- as the anion.[35]

Another intriguing aspect of the redox chemistry of this class of compounds is the formation of dimers via either one-electron oxidation of the anions in alkali-metal salts (**2**)[36, 37] or one-electron reduction of the cations (**3**).[38] Such dimeric species have so far been characterized as two distinct structural isomers; the majority of examples exist as dichalcogenide dimers (**4**) with an elongated E-E interaction.[36,37] For the *hetero*dichalcogenidoimidodiphosphinate (**2**, E ≠ E′), the resulting dimer is exclusively obtained as a ditelluride with a Te-Te interaction rather than an E-E or E-Te interaction.[38] The second bonding mode is best described as a spirocyclic contact ion pair (**5**) in which a dichalcogenido anion is chelated to one of the chalcogen atoms of the corresponding cation.[37] To date this structural type has been limited to the all-tellurium system with R = ^{t}Bu. However, DFT calculations predict that the difference in the relative energies of the two isomers **4** and **5** is small (< 20 kJ mol^{-1}) for the heavier chalcogenido derivatives (E = Se, Te; R = ^{i}Pr, ^{t}Bu).[37]

The above-mentioned one-electron redox processes are limited to the formation of dimers in which the two halves are identical. We were intrigued, therefore, to elucidate the nature of the chalcogen-chalcogen bonding in molecules in which the chalcogen atoms on one side of the molecule are different from those on the other side. To this end, we now describe the application of a new approach to the synthesis of molecules with a

central E-Te bond, namely the reaction of sodium salts of the anions $[(EPR_2)_2N]^-$ (**2**, E = S, Se; R = ^{i}Pr, ^{t}Bu; M = Na) with the cations $[(TePR_2)_2N]^+$ (**3**, E = Te; R = ^{i}Pr, ^{t}Bu) in the form of iodide salts. The products have been characterized in solution by variable temperature multinuclear NMR spectroscopy and in the solid state by single crystal X-ray crystallography, which has revealed a third structural type for these chalcogen-rich systems. The relative energies of structural isomers and the nature of chalcogen-chalcogen bonding have been probed by DFT calculations.

Results and Discussion

Synthesis and NMR spectra of 6b,c and 7b,c. The salt-elimination reactions of a TMEDA-solvated sodium salt of the dichalcogenidoimidodiphosphinate anions (E = S, Se; R = ^{i}Pr, ^{t}Bu) with the corresponding ditelluridoimidodiphosphinate cation (as its iodide salt) in toluene proceeded according to Scheme 1. After removal of NaI and recrystallization from hexane at -35 ^{o}C, the products **6b,c** and **7b,c** were obtained as air-sensitive orange-red crystals in 45-60 % yields. The use of toluene as solvent was found to be essential for the success of this synthetic approach. Initial attempts to prepare **7b** in THF led to the recovery of the reagents $[(SeP^iPr_2)_2N]Na(TMEDA)$ and $[(TeP^iPr_2)_2N]I$. This observation was subsequently attributed to the solubility of NaI in THF, since an authentic sample of **7b** (prepared in toluene) was shown to form $[(SeP^iPr_2)_2N]Na$ and $[(TeP^iPr_2)_2N]I$ in THF upon addition of NaI.

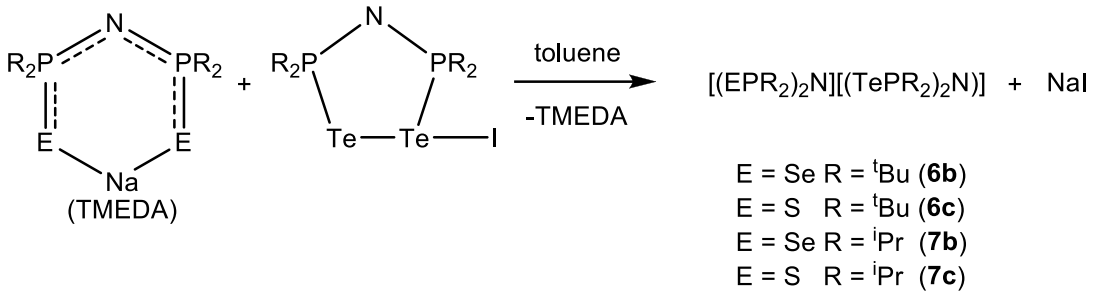

Scheme 1

^{31}P NMR spectra of the structurally disparate dimers **4** and **5** provide useful information about structures in solution in view of their characteristic chemical shifts and the magnitude of the one-bond P-E coupling constants (^{77}Se, I = ½, 7.6 %; ^{125}Te, I = ½, 7.0 %).[36-38] At low temperatures, dichalcogenides of type **4** show a pair of mutually coupled doublets corresponding to the two phosphorus environments observed in their solid-state structures.[37] By contrast, the contact ion pair **5**, which has only been characterized for the all-tellurium system (E = Te, R = ^{t}Bu) exhibits four ^{31}P phosphorus resonances at 193 K as expected for the spirocyclic structure. It should be noted, however, that the dimers **4** and **5** show fewer resonances than expected at room temperature as a result of fluxional behavior.

The ^{31}P NMR spectra of **6b,c** and **7b,c** at 293 K display only two resonances with the appropriate chalcogen satellites (see Table 2). The chemical shifts are compatible with a contact-ion pair structure rather than a dichalcogenide of the type **4**. In each case, the tellurium-bound phosphorus atoms display chemical shifts which are downfield-shifted by < 11 ppm with respect to the corresponding tellurium cations in [(TePR$_2$)$_2$N]I (R = ^{t}Bu, δ 83.5, ^{1}J(P-Te) = 959 Hz; ^{i}Pr, δ 68.1, ^{1}J(P-Te) = 1040 Hz).[34, 37] However, the *tert*-butyl derivatives **6b** and **6c** display a slightly smaller ^{1}J(P-Te) coupling constant whereas the *iso*-propyl derivatives **7b** and **7c** show a larger ^{1}J(P-Te) coupling constant

(see Table 2) compared to those in the corresponding iodide salts. The S/Se-bound phosphorus atoms of **6b,c** and **7b,c** also display chemical shifts (and ^{1}J(P-Se) coupling constants in the case of **6b** and **7b**) within close proximity to those of the Na-bound $[(EPR_2)_2N]^-$ anions (R = ^{t}Bu, E = S, δ 69.9; Se, δ 65.9, ^{1}J(P-Se) = 627 Hz; R = ^{i}Pr, E = S, δ 62.3; Se, δ 56.6, ^{1}J(P-Se) = 617 Hz).[31]

The ^{31}P NMR spectra of the *tert*-butyl derivatives **6b** and **6c** were also collected at 185 K (Table 2). The spectrum of **6b** resolves into four separate resonances while that of **6c** displays only three resonances, with one of the original resonances resolving into two while the other broadens substantially, but does not separate into two peaks. In both cases, the broadness of the resonances precludes the observation of the chalcogen satellites. By contrast, the *iso*-propyl derivatives **7b** and **7c** display four well-resolved resonances in their ^{31}P NMR spectra at 200 K. The spectrum of **7b** exhibits two resonances with ^{1}J(P-Te) coupling constants of 1045 and 1122 Hz, respectively, cf. 1108 Hz at 293 K. Only one of the other resonances displays ^{77}Se satellites (^{1}J(P-Se) = 481 Hz). The ^{77}Se satellites for the other resonance are obscured by other resonances with similar chemical shifts. The ^{31}P NMR spectrum of **7c** at 200 K also exhibits two peaks with ^{1}J(P-Te) coupling of 1056 and 1102 Hz, cf. 1079 Hz at 293 K.

In summary, while the ^{31}P NMR chemical shifts and the number of resonances observed for **6b,c** and **7b,c** are indicative of contact ion pair structures, the disparities in the values of ^{1}J(P-E) (E = Se, Te) for **6b,c** compared to **7b,c** suggest the possibility of structural differences in solution.

Crystal structures of contact ion pairs 6b,c and 7b,c. The solid-state structures of **6b,c** and **7b,c** were determined by X-ray crystallographic analyses. Pertinent bond parameters

are provided in Table 3. The structures of **6b** (Figure 1) and **6c** (Figure 2) confirmed that these chalcogen-rich systems exist as spirocyclic contact ion pairs with a similar molecular arrangement to that previously observed for the all-tellurium containing derivative **6a**, i.e. the $[EP^tBu_2NP^tBu_2E]^-$ (E = S, Se) anion is chelated via both chalcogen atoms to one tellurium atom of the $[(TeP^tBu_2)_2N]^+$ cation.[37]

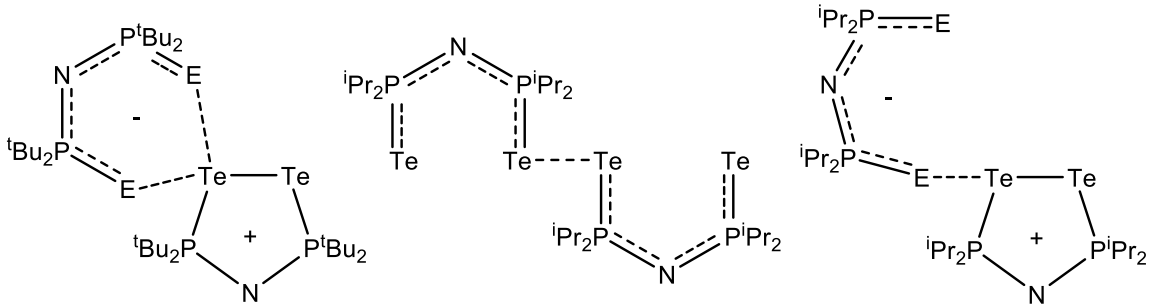

The crystal structures of the *iso*-propyl derivatives **7b** (Figure 3) and **7c** (Figure 4) also reveal contact ion pairs. However, in these systems the anion $[EP^iPr_2NP^iPr_2E]^-$ (E = S, Se) is connected to one tellurium of the $[(TeP^iPr_2)_2N]^+$ cation by a single chalcogen (E) atom, i.e. in a monodentate fashion. This arrangement represents a novel third structural isomer for molecules comprised of two dichalcogenidoimidodiphosphinates involving S, Se or Te. Indeed, only a few complexes containing a monodentate $[EPR_2NPR_2E]^-$ anion have been characterized with the majority involving asymmetric oxygen-containing ligands which bind in this fashion as a consequence of hard/soft donor mismatch.[39-41] To the best of our knowledge, the only *homo* dichalcogenidoimidodiphosphinate anions that coordinate in a monodentate fashion are found in the complexes $Te[Et_2P(S)NP(S)(OPh)_2]_2$ [42] and $\{Co[\eta^2\text{-}(OPPh_2)_2N]_2[\eta^1\text{-}OPPh_2NPh_2PO]\}$.[43] The former example can also be regarded as a distorted η^2 complex, since the "uncoordinated" sulfur

atom lies only 2.91 Å from the metal center, cf. d(S-Te) = 3.15 Å in the spirocyclic dimer **6c**. The monodentate nature of one of the ligands in the cobalt complex can possibly be explained by steric crowding of the metal center by the other two bidentate ligands. In the case of complexes **7b** and **7c**, however, steric bulk clearly does not inhibit a bidentate mode of bonding since the *tert*-butyl complexes **6a-c** accommodate a bidentate anion.

Like **6a**, the spirocyclic contact ion pairs **6b** and **6c** contain an almost linear Te-Te-E chain (**6b**, 177.45(2)^{o}; **6c**, 178.23(3)^{o}) with the central tellurium atom lying in a distorted square-planar environment (Σ < Te(1) = 360.20^{o} and 359.76^{o}, respectively), which is completed by a phosphorus atom of the PNP backbone and the other E atom of the anion. The Te-E bond distances are considerably different within each compound, with the linear-bound chalcogen atom displaying a much shorter bond to the central Te atom than the other chalcogen (E) atom. However, the former bonds are both noticeably longer (weaker) than a typical Te-E single bond;[44] their bond orders[45] and elongations (expressed as a percentage) are summarized in Table 4.

In the monodentate contact ion pairs **7b** and **7c** the coordinated E(1) atom also forms an approximately linear E-Te-Te structure (**7b**, 175.28(2)^{o}; **7c**, 173.07^{o}). A similar linear SeTeTe arrangement (176.14(1)^{o}) is evident in the contact ion pair [(R_3PSeTe*p*-Tol)$^{+}$(*p*-TolTeI_2)$^{-}$],[46] although in that case the cation-anion interaction involves the two tellurium atoms. The lack of coordination of E(2) to a tellurium center in the *iso*-propyl derivatives **7b** and **7c** allows the EPNPE backbone of the anion to adopt its preferred conformation with the terminal chalcogen atom pointing away from the cyclic cation [EPPE dihedral angle = 142.40(1)^{o} (**7b**), 141.5(1)^{o} (**7c**)]. Coordination of E(2) to Te(1) in the *tert*-butyl complexes **6b** and **6c** causes a lengthening of the P(4)-E(2) bond with

respect to complexes **7b** and **7c**, whereas the terminal E(2)-P(4) bond length more closely resembles a double bond, e.g. $(EP^iPr_2)_2NH$ [S-P = 1.95; Se-P = 2.10 Å].[47,48]

One of the most interesting features of these mono- and bidentate contact-ion pairs is the elongation of Te-Te bonds of the cationic component compared to a typical Te-Te single bond.[49] Similar to previously studied five-membered $[(EPR_2)_2N]^+$ cyclic cations,[32,36] the elongation is a direct consequence of the strength of the interaction between the cation and the anion, since donation of electron density from the anion into the σ^*(E-E) orbital (the LUMO) of the cation results in a decrease in the E-E bond order. The data in Table 4 show that there is a clear correlation between the strength of the anion-cation [E(1)-Te(1)] interaction, as manifested by the calculated bond order, and the percentage elongation of the Te-Te bond compared to a typical single-bond value.

As E(1) is changed from Te to Se and finally to S, the E-Te interaction clearly becomes weaker and, consequently, this bond is elongated (by up to 20% in the case of **6c**). The diminution of the E-Te interaction results in reduced electron donation from the anion into the LUMO of the cation so that, while the Te-Te bonds are all still elongated, this lengthening becomes less pronounced. A comparison of the bond lengths for **6b** and **7b** (or **6c** and **7c**) indicates that the cation-anion interaction is stronger when ^{i}Pr rather than ^{t}Bu groups are bound to the phosphorus atoms. While it is tempting to attribute this disparity to the identity of the organic group, the different mode of coordination (monodentate *vs* bidentate) of the anion to the cation may also be a contributing factor. Theoretical calculations performed for the different isomers support the latter explanation as the E-Te bond length is calculated to be considerably (0.02 Å) shorter in **6b** and **6c** when monodentate coordination of the anion is enforced.

Finally, there is an obvious disparity between the P-Te bond lengths in these contact ion pairs, with the Te(1)-P(1) bond being longer than the Te(2)-P(2) bond by ca. 0.15 Å for **6b** and **6c** and 0.06-0.07 Å for **7b** and **7c**. This observation, which is also apparent in the structure of **6a**,[37] is consistent with the difference of 45-80 Hz in the ^{1}J(P-Te) coupling constants for **7b** and **7c** at low temperature.

Theoretical Investigations of Structural Isomers of 6 and 7. DFT level geometry optimizations were performed for **6b** and **7b** as well as for **6c** and **7c**. Pertinent optimized structural parameters are listed in Table 3; the calculated geometries of **6a** and **7a** have been reported in an earlier publication.[37] There is a quite good agreement between the theoretical and experimental results, the most notable discrepancies being observed in the bond lengths involving the Te(1) center. In general, DFT calculations overestimate the anion-cation interaction and concomitantly give E-Te(1) and Te(1)-Te(2) bond lengths which are too short and long, respectively. This is most apparent in case of **7b** and **7c** which coordinate in a monodentate fashion and for which the difference in bond lengths is as much as ±0.10 Å. Nevertheless, the trends in optimized structural parameters parallel the data from X-ray structural determinations.

The observed preference of **6b,c** and **7b,c** to adopt a contact ion pair structure can be explained by the apparent weakness of the E-Te (E = S, Se) bond which would be formed in the dichalcogenide alternative. As noted earlier, the known heterodichalcogenide dimers are exclusively obtained as ditellurides.[38] However, it is not as straightforward to rationalize why **7b** and **7c** adopt a monodentate coordination mode. To investigate this further, we performed geometry optimizations for **6a**-**c** and **7b**,**c** using monodentate structures for the former and bidentate for the latter. An energetic

comparison between the two isomers shows that the *tert*-butyl derivatives **6a-c** favor the bidentate coordination mode by a clear margin, approximately 35-45 kJ mol^{-1}. Interestingly, the bidentate coordination mode is more favorable also for **7b** and **7c** though the energetic preference is less clear, 10 and 5 kJ mol^{-1} for the former and latter, respectively. This indicates that crystal packing effects might play a role in stabilizing the monodentate structure. Indeed, the X-ray structure of **7b** displays several short intermolecular contacts involving the dangling chalcogen center, whereas none are observed for the *tert*-butyl analogue **6b**.

The charge distributions in **6** and **7** were examined by calculating the molecular electrostatic potentials (ESPs) and plotting the results on molecular van der Waals surfaces, i.e. surfaces for which the total electron density equals 0.001 a.u. The results are shown in Figure 5 for **6c** and **7c**; the distributions for the corresponding selenium and tellurium systems are qualitatively similar to the given data and deserve no further discussion. As evident from Figure 5, the anionic and cationic halves of the structures can be easily identified and the description of **6a-c** and **7b-c** as contact ion pairs is clearly warranted. In both isomers, the E(2) atom bears a significant local charge concentration. This is particularly visible in the monodentate structure in which the E(2) chalcogen atom remains uncoordinated and is surrounded by a negative charge cloud. This is not unexpected considering the shape of the HOMO in the anions, which corresponds to the σ^*(E-E) LUMO of cation.[34,35]

The amount of charge transferred from the anion to the cation can be estimated by summing the atomic partial charges within the two halves of the contact ion pair structure; the calculated values are given in Table 4. As expected, the observed trend

parallels the trend seen in Te(1)-Te(2) bond lengths. In both sets **6** and **7**, the sum of atomic charges (in absolute sense) decreases in the order S > Se > Te, indicating greatest charge transfer for **6a** and, hence, the longest Te(1)-Te(2) bond length. We note that the charges reported in Table 4 were obtained by employing the natural population analysis, but the trend is reproducible using *e.g.* Mulliken or Hirschfield approaches. However, the absolute values given by each method are expected to differ considerably. Different computational approaches give rise to vastly different values for atomic properties since they use different criteria to divide the total electron density between atoms in a molecule. Hence, it is best not to put too much weight on absolute values, but instead look at the predicted trends.

An interesting question which remains unanswered is whether it would be possible to form contact ion pair structures like 6 in which the identities of the anions and cations are reversed. This can be investigated computationally by calculating (adiabatic) ionization energies (IEs) and electron affinities (EAs) for the neutral molecules $(EPR_2)_2N$ (E = S, Se, Te). The results (Table 5) for the *iso*-propyl and *tert*-butyl series show that both the EA and IE decrease in the order S > Se > Te, i.e. energetic factors favor the formation of the tellurium cation and sulfur (selenium) anion. The same conclusion is reached if energies for different cation-anion pairs are calculated by summing the energies of the free ions in the gas phase; the contribution from the E-Te bond should be essentially equal in the two alternatives. Thus, these simple arguments imply that that synthetic approaches utilizing the cations $[(EPR_2)_2N]^+$ (E = S, Se) with the tellurium anions $[(TePR_2)_2N]^-$ would yield exactly the same products as reported in the current contribution.

Conclusions

In an earlier publication[37] we raised the possibility of "preparing other spirocyclic contact ion pairs or mixed chalcogen (dimeric) systems by the reactions of an acyclic $[(EPR_2)_2N]^-$ anion with a cyclic $[(E'PR_2)_2N]^+$ cation ($E \neq E'$)." In this work we have demonstrated the viability of this synthetic approach and shown that it gives rise to contact ion pairs in the form of two structural isomers depending on the nature of the substituents attached to phosphorus. DFT calculations reveal that the energy difference between the monodentate and bidentate contact ion pairs is very small for structures with *iso*-propyl substituents and help to rationalize the observed structural trends. The strength of the interaction between the two halves of these mixed chalcogen systems largely determines the length of the Te-Te bond in the incipient cation as a result of electron donation from the anion into the LUMO [σ^*(E-E)] of the cation.

Experimental Section

General Procedures. All reactions and manipulations of products were performed under an argon atmosphere by using standard Schlenk techniques or an inert atmosphere glovebox. The reagents $(EP^iPr_2)_2NNa(TMEDA)$ (E = S, Se),[19] $(EP^tBu_2)_2NNa(TMEDA)$ (E = S, Se),[37] $[(TeP^iPr_2)_2N]I$[34] and $[(TeP^tBu_2)_2N]I$[37] were prepared by literature methods. The solvents toluene, *n*-hexane and tetrahydrofuran (THF) were dried by distillation over Na/benzophenone and stored over molecular sieves under an argon atmosphere prior to use.

Spectroscopic Methods. ^{31}P NMR spectra were obtained in THF-d_8 on a Bruker DRX 400 spectrometer operating at 161.765 MHz and were referenced externally to an 85%

solution of H_3PO_4 in D_2O. Elemental analyses were performed by Analytical Services, Department of Chemistry, University of Calgary, Calgary, Canada.

Synthesis of [(SeP^{t}Bu$_2$)$_2$N][(TeP^{t}Bu$_2$)$_2$N] (**6b**). A solution of (SeP^{t}Bu$_2$)$_2$NNa(TMEDA) (0.088 g, 0.146 mmol) in toluene (20 mL) was added via cannula to a solution of [(TeP^{t}Bu$_2$)$_2$N]I (0.100 g, 0.146 mmol) in toluene (20 mL) and this was allowed to stir for 1 hour. Toluene (and TMEDA) was removed *in vacuo* and the remaining solid was redissolved in hexane (25 mL). This was filtered through Celite to remove NaI and concentrated to approx 2 mL in vacuo. After ca. 1 h at -35 ^{o}C, red crystals (0.068 g, 46 %) had precipitated. Anal. Calcd (%) for $Se_2Te_2P_4N_2C_{32}H_{72}$: C, 37.61; H, 7.10; N, 2.74. Found: C, 37.99; H, 7.21; N, 2.63. $^{31}P\{^1H\}$ NMR (THF-d$_8$, 293 K) δ = 72.6 (s, ^1J(P-Te) = 945 Hz), 69.7 (s, ^1J(P-Se) = 611 Hz). $^{31}P\{^1H\}$ NMR (THF-d$_8$, 185 K) δ = 77.4 (s), 72.7 (s), 67.6 (s), 64.4 (s).

Synthesis of [(SP^{t}Bu$_2$)$_2$N][(TeP^{t}Bu$_2$)$_2$N] (6c). The salt **6c** was obtained as dark red crystals (0.084 g, 62 %) from the reaction of (SP^{t}Bu$_2$)$_2$NNa(TMEDA) (0.074 g, 0.146 mmol) and [(TeP^{t}Bu$_2$)$_2$N]I (0.100 g, 0.146 mmol) by using a procedure identical to that described above for **6b**. Anal. Calcd (%) for $S_2Te_2P_4N_2C_{32}H_{72}$: C, 41.41; H, 7.81; N, 3.02. Found: C, 41.70; H, 7.87; N, 3.11. $^{31}P\{^1H\}$ NMR (THF-d$_8$, 293 K) δ = 77.8 (s, ^1J(P-Te) = 928 Hz), 70.4 (s). $^{31}P\{^1H\}$ NMR (THF-d$_8$, 185 K) δ = 77.8 (br s), 69.9 (s), 68.2 (s).

Synthesis of [(SeP^{i}Pr$_2$)$_2$N][(TeP^{i}Pr$_2$)$_2$N] (**7b**)**.** The salt **7b** was obtained as orange-red crystals (0.089 g, 61 %) from the reaction of (SeP^{i}Pr$_2$)$_2$NNa(TMEDA) (0.087 g, 0.160 mmol) and [(TeP^{i}Pr$_2$)$_2$N]I (0.101 g, 0.160 mmol) by using a procedure identical to that described above for **6b**. Anal. Calcd (%) for $Se_2Te_2P_4N_2C_{24}H_{56}$: C, 31.69; H, 6.20; N,

3.08. Found: C, 32.26; H, 6.06; N, 3.05. $^{31}P\{^{1}H\}$ NMR (THF-d_8, 293 K) δ = 61.9 (s, ^{1}J(P-Te) = 1108 Hz), 57.8 (s, ^{1}J(P-Se) = 564 Hz). $^{31}P\{^{1}H\}$ NMR (THF-d_8, 200 K) δ = 66.9 (s, ^{1}J(P-Te) = 1045 Hz), 61.2 (s, ^{1}J(P-Se) = 505 Hz), 59.7 (s, ^{1}J(P-Te) = 1122 Hz) 52.6 (s, ^{1}J(P-Se) = 481 Hz).

Synthesis of [(SP^{i}Pr$_2$)$_2$N][(TeP^{i}Pr$_2$)$_2$N] (7c). The salt **7c** was obtained as orange crystals (0.065 g, 51 %) from the reaction of (SP^{i}Pr$_2$)$_2$NNa(TMEDA) (0.071 g, 0.157 mmol) and [(TeP^{i}Pr$_2$)$_2$N]I (0.099 g, 0.157 mmol) by using a procedure identical to that described above for **6b**. Anal. Calcd (%) for $S_2Te_2P_4N_2C_{24}H_{56}$: C, 35.33; H, 6.92; N, 3.43. Found: C, 36.13; H, 6.83; N, 3.25. $^{31}P\{^{1}H\}$ NMR (THF-d_8, 293 K) δ = 63.6 (s, ^{1}J(P-Te) = 1079 Hz), 59.9 (s). $^{31}P\{^{1}H\}$ NMR (THF-d_8, 185 K) δ = 70.6 (s, ^{1}J(P-Te) = 1056 Hz), 64.1 (s), 62.6 (s, ^{1}J(P-Te) = 1102 Hz), 56.0 (s).

X-ray Crystallography. Crystals of **6b**, **6c**, **7b** and **7c** were coated with Paratone 8277 oil and mounted on a glass fiber. Diffraction data were collected on a Nonius KappaCCD diffractometer using Mo Kα radiation (λ = 0.71073 Å) at -100 ^{o}C. The unit-cell parameters were calculated and refined from the full data set. Crystal cell refinement and data reduction were carried out using the Nonius *DENZO* package. After data reduction, the data were corrected for absorption based on equivalent reflections using *SCALEPACK* (Nonius, 1998). All structures were solved by Patterson techniques using *SHELXS-97*,[50] while refinements were carried out on F^2 against all independent reflections by the full-matrix least-squares method by using the *SHELXL-97* program.[51] The H atoms were calculated geometrically and were riding on their respective atoms, and all non-H atoms were refined with anisotropic thermal parameters. Crystallographic data are summarized in Table 1.

Computational Details. DFT calculations were performed for different structural isomers of compounds **6** and **7** (see text for details). The calculations included the R-substituents and molecular structures were fully optimized by using a combination of the PBE exchange-correlation functional[52-54] with the Ahlrichs' triple-zeta valence basis sets augmented by one set of polarization functions (def-TZVP);[55] for tellurium the corresponding ECP basis set was used.[56] Atomic charges were obtained by performing natural population analysis on optimized structures.[57] All calculations were performed with the Turbomole 5.10 program package.[58] Visualizations for Figure 5 were done with the gOpenMol program.[59, 60]

Acknowledgment. The authors gratefully acknowledge the Natural Sciences and Research Council (Canada) (SDR and TC) and the Academy of Finland (HMT) for financial support.

Supporting Information Available: X-ray crystallographic files in CIF format. This material is available free of charge via the Internet at http://pubs.acs.org

References

1. Schmidpeter, A.; Böhm, R, Groeger, H. *Angew. Chem. Int. Ed.* **1964**, *3*, 704.
2. Schmidpeter, A.; Groeger, H. *Z. Anorg. Allg. Chem.* **1966**, *345*, 106.
3. Ly, T.Q.; Woollins, J.D. *Coord. Chem. Rev*. **1998**, *176*, 451.
4. Silvestru, C; Drake, J.E. *Coord. Chem. Rev*. **2001**, *223*, 117.
5. Haiduc, I. *Compr. Coord. Chem. II*, **2004**, 323.
6. Afzaal, M.; Aucott, S.M.; Crouch, D.; O'Brien, P.; Woollins, J.D.; Park, J.-H. *Chem. Vap. Deposition* **2002**, *8*, 187.
7. Park, J.-H.; Afzaal, M.; Helliwell, M.; Malik, M.A.; O'Brien, P.; Raftery, J. *Chem. Mater*. **2003**, *15*, 4205.
8. Crouch, D.; Helliwell, M.; O'Brien, P.; Waters, J.; Williams, D.J. *Dalton Trans*. **2003**, 1500.
9. Afzaal, M.; Crouch, D.; Malik, M.A.; Motevalli, M.; O'Brien, P.; Park, J.-H. *J. Mater. Chem*. **2003**, *13*, 639.
10. Crouch, D.J.; Hatton, P.M.; Helliwell, M.; O'Brien, P.' Raftery, J. *Dalton Trans*. **2003**, 2761.
11. Afzaal, M.; Crouch, D.J.; O'Brien, P.; Raftery, J; Skabara, P.J.; White, A.J.P.; Williams, D.J. *J. Mater. Chem*. **2004**, *14*, 233.
12. Afzaal, M.; Ellwood, K.; Pickett, N.L.; O'Brien, P.; Raftery, J.; Waters, J. *J. Mater. Chem*. **2004**, *14*, 1310.
13. Waters, J.; Crouch, D.; Raftery, J., O'Brien, P. *Chem. Mater.* **2004**, *16*, 3289.
14. Afzaal, M.; Crouch, D.; Malik, M.A.; Motevalli, M.; O'Brien, P.; Park, J.-H.; Woollins, J.D. *Eur. J. Inorg. Chem.* **2004**, *1*, 171.
15. Afzaal, M.; Crouch, D.; O'Brien, P. *Mater. Sci. Eng. B.* **2005**, *116*, 391.
16. Panneerselvam, A.; Malik, M.A.; Afzaal, M.; O'Brien, P.; Helliwell, M. *J. Am. Chem. Soc.* **2008**, *130*, 2420.
17. Panneerselvam, A.; Nguyen, C.Q.; Waters, J.; Malik, M.A.; O'Brien, P.; Raftery, J.; Helliwell, M. *Dalton Trans.* **2008**, 4499.
18. Crouch, D.J.; O'Brien, P.; Malik, M.A.; Skabara, P.J.; Wright, S.P. *Chem. Commun*. **2003**, 1454.

19. Briand, G.G.; Chivers, T.; Parvez, M. *Angew. Chem. Int. Ed*. **2002**, *41*, 3468.
20. Chivers, T.; Eisler, D.J.; Ritch, J.S. *Dalton. Trans*. **2005**, 2675.
21. Copsey, M.C.; Chivers, T. *Chem. Commun.* **2005**, 4938.
22. Copsey, M.C.; Panneerselvam, A.; Afzaal, M.; Chivers, T.; O'Brien, P. *Dalton Trans*. **2007**, 1528.
23. Levesanos, N.; Robertson, S.D.; Maganas, D; Raptopoulou, C.P.; Terzis, A.; Kyritsis, P.; Chivers, T. *Inorg. Chem.* **2008**, *47*, 2949.
24. Eisler, D.J.; Robertson, S.D.; Chivers, T. *Can. J. Chem*. **2009**, *87*, 39.
25. Gaunt, A.J.; Scott, B.L.; Neu, M.P. *Angew. Chem. Int. Ed.* **2006**, *45*, 1638.
26. Gaunt, A.J.; Reilly, S.D.; Enriquez, A.E.; Scott, B.L.; Ibers, J.A.; Sekar, P.; Ingram, K.I.M.; Kaltsoyannis, N.; Neu, M.P. *Inorg. Chem.* **2008**, *47*, 29.
27. Garje, S.S.; Ritch, J.S.; Eisler, D.J.; Afzaal, M.; O'Brien, P.; Chivers, T. *J. Mater. Chem.* **2006**, *16*, 966.
28. Garje, S.S.; Copsey, M.C.; Afzaal, M.; O'Brien, P.; Chivers, T. *J. Mater. Chem*. **2006**, *16*, 4542.
29. Garje, S.S.; Eisler, D.J.; Ritch, J.S.; Afzaal, M.; O'Brien, P.; Chivers, T. *J. Am. Chem. Soc.* **2006**, *128*, 3120.
30. Ritch, J. S.; Ahmad, K.; Afzaal, M.; Chivers, T.; O'Brien, P. *J. Am. Chem. Soc.* submitted for publication.
31. Robertson, S.D.; Chivers, T. *Dalton Trans.* **2008**, 1765.
32. Robertson, S.D.; Chivers, T.; Akhtar, J.; Afzaal, M.; O'Brien, P. *Dalton Trans.* **2008**, 7004.
33. Robertson, S.D.; Ritch, J.S.; Chivers, T. *Dalton Trans*. **2009**, to be submitted.
34. Konu, J.; Chivers, T.; Tuononen, H.M. *Chem. Commun.* **2006**, 1634.
35. Konu, J.; Chivers, T.; Tuononen, H.M. *Inorg. Chem.* **2006**, *45*, 10678.
36. Chivers, T.; Eisler, D.J.; Ritch, J.S.; Tuononen, H.M. *Angew. Chem. Int. Ed*. **2005**, *44*, 4953.
37. Ritch, J.S.; Chivers, T.; Eisler, D.J.; Tuononen, H.M. *Chem. Eur. J.* **2007**, *13*, 4643.
38. Robertson, S.D.; Chivers, T.; Tuononen, H.M. *Inorg. Chem.* **2008**, *47*, 10634.

39. Slawin, A.M.Z.; Smith, M.B.; Woollins, J.D. *J. Chem. Soc. Dalton Trans.* **1998**, 1537.
40. Slawin, A.M.Z.; Smith, M.B. *New J. Chem.* **1999**, *23*, 777.
41. Smith, M.B.; Slawin, A.M.Z. *Polyhedron*, **2000**, *19*, 695.
42. Birdsall, D.J.; Novosad, J.; Slawin, A.M.Z.; Woollins, J.D. *J. Chem. Soc. Dalton Trans.* **2000**, 435.
43. Ellermann, J.; Bauer, W.; Dötzler, M.; Heinemann, F.W.; Moll, M. *Monatsh. Chem.* **1999**, *130*, 1419.
44. Pauling, L. *The Nature of the Chemical Bond*, 3rd ed.; Cornell University Press: Ithaca, NY, 1960.
45. The bond orders were calculated by the Pauling equation $N = 10^{(D-R)/0.71}$ where R is the observed bond length (Å). The single bond length D is estimated from the sums of appropriate covalent radii (Å):[44] Te-S 2.41, Te-Se 2.54, Te-Te 2.74.
46. Hrib, C.G.; Jeske, J.; Jones, P.G.; du Mont, W.-W. *Dalton Trans.* **2007**, 3483.
47. Cupertino, D.; Keyte, R.W.; Slawin, A.M.Z.; Williams, D.J.; Woollins, J.D. *Inorg. Chem.* **1996**, *15*, 4441.
48. Cupertino, D.; Birdsall, D.J.; Slawin, A.M.Z.; Woollins, J.D. *Inorg. Chim. Acta* **1999**, *290*, 1.
49. For example, the Te-Te bond of PhTe-TePh is 2.71 Å. Llabres, P.G.; Dideberg, O.; Dupont, L. *Acta Cryst.* **1972**, *B28*, 2438.
50. Sheldrick, G.M. *SHELXS-97, Program for Crystal Structure Determination*, University of Göttingen: Gottingen, Germany, 1997.
51. Sheldrick, G.M. *SHELXS-97, Program for Crystal Structure Refinement*, University of Göttingen: Göttingen, Germany, 1997.
52. Perdew, J. P.; Burke, K.; Ernzerhof, M. *Phys. Rev. Lett.* **1996**, *77*, 3865.
53. Perdew, J. P.; Burke, K.; Ernzerhof, M. *Phys. Rev. Lett.* **1997**, *78*, 1396.
54. Perdew, J. P.; Burke, K.; Ernzerhof, M. *J. Chem. Phys.* **1996**, *105*, 9982.
55. Schäfer, A.; Huber, C.; Ahlrichs, R. *J. Chem. Phys.* **1994**, *100*, 5829.
56. Bergner, A.; Dolg, M.; Kuechle, W.; Stoll, H.; Preuss, H. *Mol. Phys.* **1993**, *80*, 1431.

57. Reed, A. E.; Weinstock, R. B.; Weinhold, F. *J. Chem. Phys.* **1985**, *83*, 735.

58. TURBOMOLE, Program Package for *ab initio* Electronic Structure Calculations, Version 5.10, TURBOMOLE GmbH, Germany, 2008. Ahlrichs, R.; Bär, M.; Häser, M.; Horn, H.; Kölmel, C. *Chem. Phys. Letters* **1989**, *162*, 1659.

59. Laaksonen, L. *J. Mol. Graph.* **1992**, *10*, 33.

60. Bergman, D. L.; Laaksonen, L.; Laaksonen, A. *J. Mol. Graph. Model.* **1997**, *15*, 301.

Captions to Figures

Figure 1. Thermal ellipsoid plot of **6b** (50% probability). All H atoms have been omitted for clarity.

Figure 2. Thermal ellipsoid plot of **6c** (50% probability). All H atoms have been omitted for clarity.

Figure 3. Thermal ellipsoid plot of **7b** (50% probability). All H atoms have been omitted for clarity.

Figure 4. Thermal ellipsoid plot of **7c** (50% probability). All H atoms have been omitted for clarity.

Figure 5. Molecular electrostatic potentials for **6c** (left) and **7c** (right). Color code: blue (negative) – green (neutral) – yellow (positive).

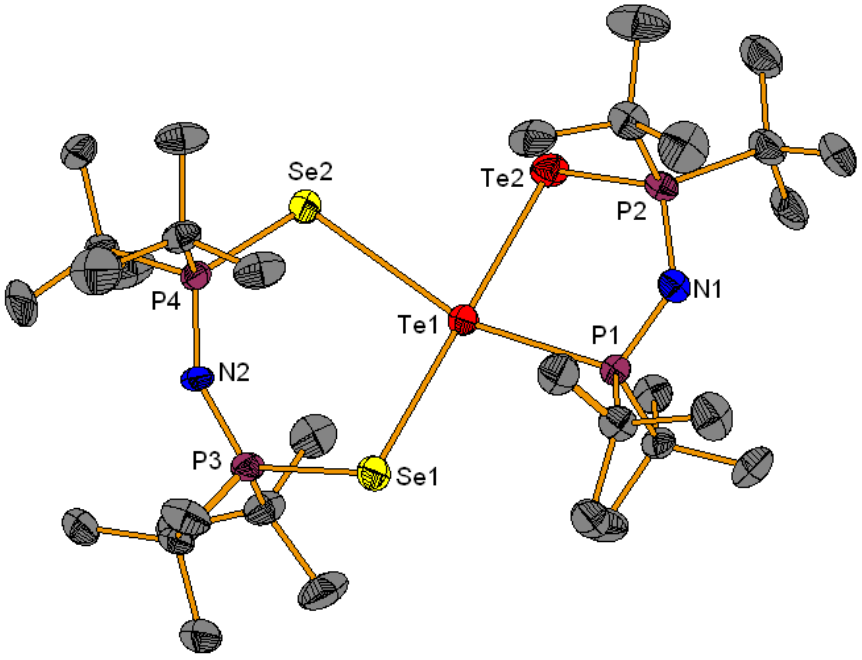

Figure 1.

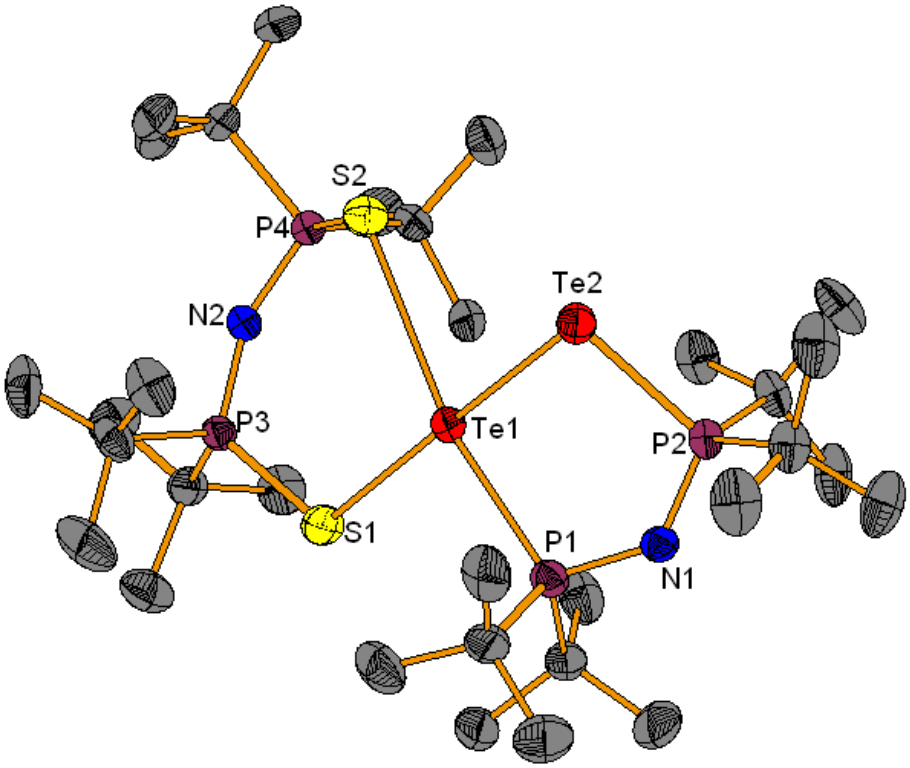

Figure 2.

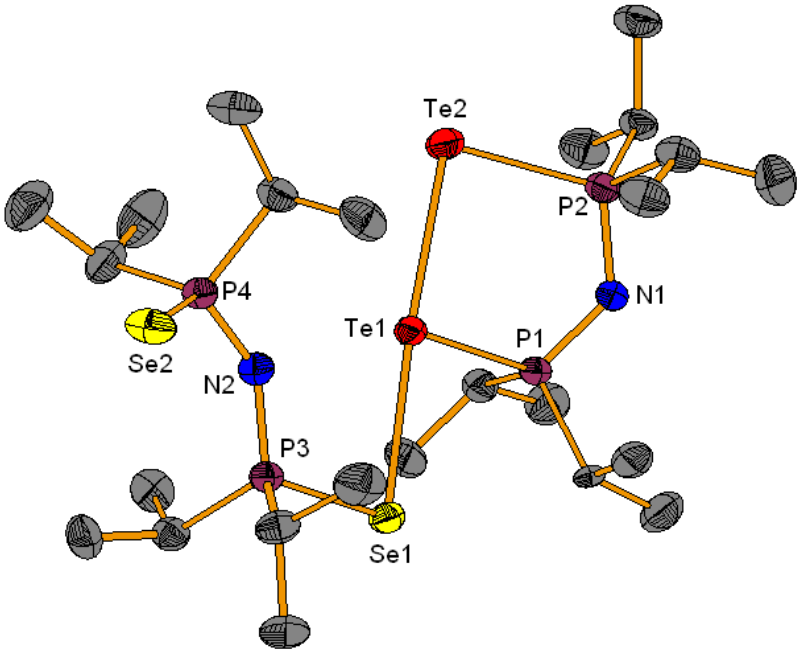

Figure 3.

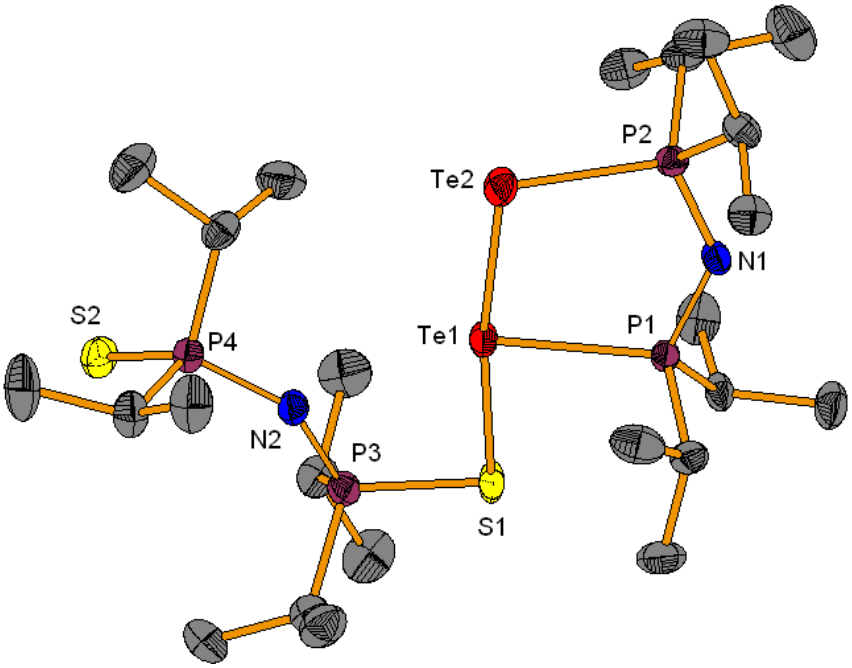

Figure 4.

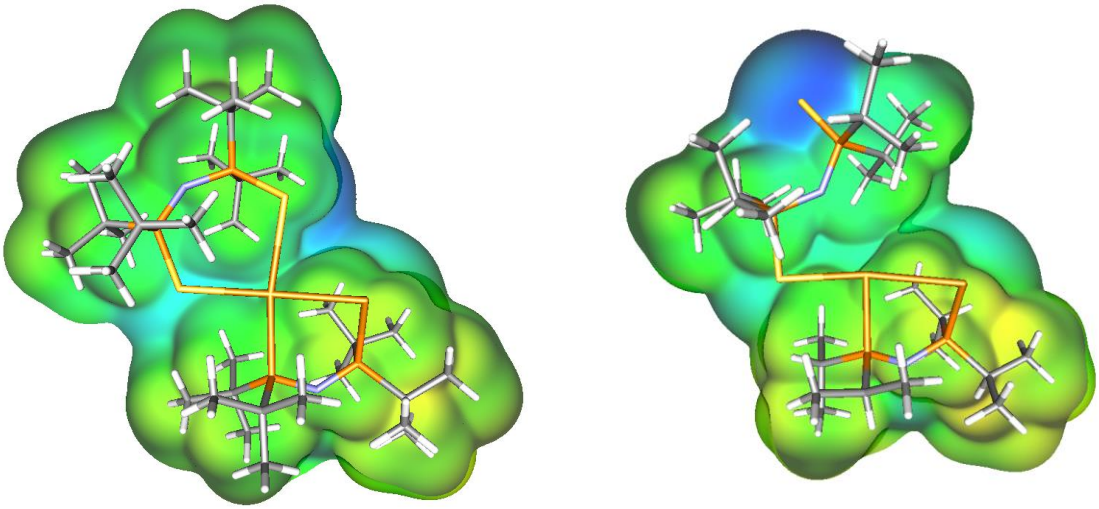

Figure 5.

Table 1. Crystallographic data for **6b**, **6c**, **7b** and **7c**[a]

	6b	**6c**	**7b**	**7c**
empirical formula	$C_{32}H_{72}N_2P_4Se_2Te_2$	$C_{32}H_{72}N_2P_4S_2Te_2$	$C_{24}H_{56}N_2P_4Se_2Te_2$	$C_{24}H_{56}N_2P_4S_2Te_2$
fw	1021.92	928.12	909.71	815.91
cryst syst	Monoclinic	Monoclinic	Monoclinic	Monoclinic
space group	P2(1)/c	P2(1)/c	P2(1)/n	P2(1)/n
a, Å	20.0789(6)	16.4711(6)	10.642(2)	8.2161(2)
b, Å	13.5947(5)	14.2349(3)	22.718(5)	22.9175(5)
c, Å	16.6720(3)	18.8467	15.812(3)	19.1012(4)
α, °	90	90	90	90
β, °	104.437(2)	97.202(1)	108.08(3)	93.521(1)
γ, °	90	90	90	90
V, Å^3	4407.2(2)	4384.0(2)	3634.0(14)	3589.8(1)
Z	4	4	4	4
T, °C	173	173	173	173
ρ_{calcd}, g/cm^3	1.540	1.406	1.663	1.510
μ (Mo Kα) mm^{-1}	3.143	1.595	3.801	1.936
cryst size, mm	0.12 x 0.12 x 0.04	0.12 x 0.12 x 0.12	0.28 x 0.06 x 0.06	0.16 x 0.04 x 0.04
F(000)	2040	1896	1784	1640
θ range, deg	2.36-25.02	2.61-25.03	2.70-25.02	1.39-27.50
reflns collected	40382	35602	45208	29017
unique reflns	7768	7736	6400	8236
R_{int}	0.1048	0.0774	0.1125	0.0745
R1 [$I > 2\sigma(I)$] [b]	0.0502	0.0418	0.0474	0.0436
wR2 (all data) [c]	0.1058	0.0987	0.1016	0.0951
GOF on F^2	1.072	1.030	1.030	1.022
completeness	99.9	99.9	99.8	99.6

[a] λ (Mo Kα) = 0.71073 Å. [b] $R1 = \Sigma||F_o|-|F_c||/\Sigma|F_o|$. [c] $wR2 = [\Sigma w(F_o^2-F_c^2)^2/\Sigma wF_o^4]^{1/2}$

Table 2. ^{31}P NMR chemical shifts and ^1J(P-E) coupling constants for **6b**, **6c**, **7b** and **7c** at 293 K and low temperature

	293 K	LT[a]
6b	72.6 (945) 69.7 (611)	77.4 72.7 67.6 64.4
6c	77.8 (928) 70.4	77.8 69.9 68.2
7b	61.9 (1108) 57.8 (564)	66.9 (1045) 61.2 (hidden) 59.7 (1122) 52.6 (481)
7c	63.6 (1079) 59.9	70.6 (1056) 64.1 62.6 (1102) 56.0

[a] Low temperature data were collected at 185 K for **6b** and **6c** and at 200 K for **7b** and **7c**.

Table 3. Selected bond lengths (Å) and angles (°) for **6b**, **6c**, **7b** and **7c**[a]

	6b (E = Se)	**6c** (E = S)	**7b** (E = Se)	**7c** (E = S)
Te(1)-Te(2)	2.922(1) [2.967]	2.868(1) [2.930]	2.958(1) [3.081]	2.940(1) [3.077]
Te(1)-P(1)	2.588(2) [2.642]	2.587(1) [2.622]	2.511(1) [2.531]	2.503(1) [2.528]
Te(2)-P(2)	2.435(2) [2.437]	2.439(1) [2.462]	2.441(2) [2.430]	2.439(1) [2.434]
P(1)-N(1)	1.612(6) [1.643]	1.619(4) [1.640]	1.591(5) [1.623]	1.595(3) [1.624]
P(2)-N(1)	1.594(6) [1.622]	1.596(4) [1.628]	1.606(5) [1.629]	1.602(3) [1.624]
Te(1)-E(1)	2.964(1) [2.944]	2.893(1) [2.866]	2.865(1) [2.784]	2.786(1) [2.681]
Te(1)-E(2)	3.156(1) [3.126]	3.150(1) [3.037]	-	-
E(1)-P(3)	2.212(2) [2.135]	2.031(2) [2.072]	2.208(2) [2.244]	2.040(2) [2.087]
E(2)-P(4)	2.165(2) [2.191]	1.998(2) [2.030]	2.129(2) [2.143]	1.974(2) [1.989]
P(3)-N(2)	1.572(6) [1.606]	1.576(4) [1.607]	1.587(5) [1.604]	1.585(3) [1.686]
P(4)-N(2)	1.612(6) [1.626]	1.604(4) [1.626]	1.609(5) [1.658]	1.608(3) [1.639]
Te(1)-P(1)-N(1)	107.4(2) [110.1]	108.3(2) [110.1]	112.5(2) [113.8]	112.8(1) [113.5]
Te(2)-P(2)-N(1)	110.1(2) [111.7]	109.9(2) [111.3]	111.8(2) [113.1]	110.8(1) [112.9]
P(1)-N(1)-P(2)	134.1(4) [131.8]	132.1(2) [130.5]	128.6(3) [127.5]	131.2(2) [129.0]
Te(1)-Te(2)-P(2)	88.30(5) [89.3]	89.08(3) [89.5]	88.98(4) [87.9]	89.91(3) [87.7]
Te(2)-Te(1)-P(1)	86.11(4) [85.0]	86.01(3) [85.5]	83.36(4) [82.0]	84.85(3) [86.3]
Te(2)-Te(1)-E(1)	177.45(2) [179.1]	178.23(3) [179.1]	175.28(2) [172.9]	173.07(2) [172.0]
Te(2)-Te(1)-E(2)	78.75(1) [83.6]	85.64(3) [85.2]	-	-
P(1)-Te(1)-E(1)	95.21(5) [94.11]	94.12(4) [93.6]	91.97(4) [91.6]	88.42(3) [88.7]
P(1)-Te(1)-E(2)	163.61(3) [168.6]	168.45(4) [170.8]	-	-
E(1)-Te(1)-E(2)	100.13(1) [97.2]	93.99(4) [95.6]	-	-
Te(1)-E(1)-P(3)	102.51(6)	110.71(6)	88.97(5)	93.21(5)

	[106.6]	[109.2]	[88.9]	[92.3]
E(1)-P(3)-N(2)	119.8(2) [119.6]	120.7(1) [119.7]	110.5(2) [107.4]	110.7(1) [107.3]
E(2)-P(4)-N(2)	119.1(2) [118.1]	119.0(2) [119.0]	117.5(2) [118.3]	117.6(1) [118.2]
P(3)-N(2)-P(4)	151.0(4) [145.7]	148.2(4) [144.6]	138.9(3) [134.9]	139.1(2) [134.2]
Te(1)-P(1)-P(2)-Te(2)	28.40(6) [27.2]	28.50(4) [26.9]	28.46(1) [30.6]	24.9(1) [28.9]
E(1)-P(3)-P(4)-E(2)	51.43(1) [50.8]	47.75(9) [49.6]	142.40(1) [146.8]	141.5(1) [146.6]

[a] Calculated values are reported in square brackets.

Table 4. Bond orders, bond elongations (in parenthesis) and sum of calculated atomic charges in **6b**, **6c**, **7b** and **7c**

	6a (E = Te)	**6b** (E = Se)	**6c** (E = S)	**7a** (E = Te)	**7b** (E = Se)	**7c** (E = S)
E(1)-Te(1)	0.309 (13.2 %)	0.253 (16.7 %)	0.209 (20.0 %)	0.513 (7.5 %)	0.349 (12.8 %)	0.295 (15.6 %)
E(2)-Te(1)	0.189 (18.7 %)	0.136 (24.3 %)	0.091 (30.7 %)	-	-	-
Te(1)-Te(2)	0.457 (8.8 %)	0.554 (6.6 %)	0.660 (4.7 %)	-	0.493 (8.0 %)	0.523 (7.3 %)
Σ(atomic charge)	± 0.20	± 0.39	± 0.50	-	± 0.43	± 0.50

Table 5. Adiabatic ionization energies (IE) and electron affinities (EA) [kJ mol^{-1}] calculated for the neutral dichalcogenides $(EPR_2)_2N$ (E = S, Se, Te; R = ^{i}Pr, ^{t}Bu)

	E = S		E = Se		E = Te	
	^{i}Pr	^{t}Bu	^{i}Pr	^{t}Bu	^{i}Pr	^{t}Bu
IE	543	524	534	513	520	498
EA	280	295	252	263	230	233